


ENDOSCOPY

Dynamic diagnosis of early gastric cancer with microvascular blood flow rate using magnifying endoscopy (with video): A pilot study

Hiroya Ueyama,*  Noboru Yatagai,* Atsushi Ikeda,* Yoichi Akazawa,* Hiroyuki Komori,* Tsutomu Takeda,* Kohei Matsumoto,* Kumiko Ueda,* Kenshi Matsumoto,* Daisuke Asaoka,* Mariko Hojo,* Takashi Yao[†] and Akihito Nagahara*

*Department of Gastroenterology, Juntendo University School of Medicine, and [†]Department of Human Pathology, Juntendo University Graduate School of Medicine, Tokyo, Japan

Key words

Blood flow rate, Blue laser imaging, Early gastric cancer, Magnifying endoscopy.

Accepted for publication 1 February 2021.

Correspondence

Dr Hiroya Ueyama, Department of Gastroenterology, Juntendo University School of Medicine, 2-1-1 Hongo, Bunkyo-Ku, Tokyo 113-8421, Japan.
Email: psyro@juntendo.ac.jp

Declaration of conflict of interest: No author has a financial relationship relevant to this publication.

Author contribution: H. Ueyama and A. Nagahara conceived and designed the study and wrote, edited, and reviewed the manuscript (conception and design). T. Yao performed all the histopathological diagnoses (analysis and interpretation of the data). N. Yatagai, A. Ikeda, Y. Akazawa, H. Komori, T. Takeda, Kohei Matsumoto, K. Ueda, Kenshi Matsumoto, and M. Hojo gathered the ME videos and patients' clinical information (analysis and interpretation of the data). H. Ueyama and A. Nagahara take full responsibility for the work as a whole, including the study design, access to data, and the decision to submit and publish the manuscript. All authors gave final approval for publication.

Introduction

White-light endoscopy is the most sensitive method for early detection of gastric cancer.¹ However, accurate diagnosis of early gastric cancer (EGC) is sometimes difficult with white-light endoscopy alone, especially for small lesions. Magnifying endoscopy with blue laser imaging (M-BLI) and magnifying endoscopy with narrowband imaging (M-NBI) are recently developed, image-enhanced endoscopic techniques.^{2,3} M-BLI and M-NBI are capable of distinguishing between EGC and non-cancer during the diagnosis of EGC by magnifying endoscopy

Abstract

Background and Aim: Magnifying endoscopy (ME) diagnostic algorithm for early gastric cancer (EGC) relies on qualitative features such as microvascular (MV) architecture and microsurface structure; however, it is a “static” diagnostic algorithm that uses still images. ME can visualize red blood cell flow within subepithelial microvessels in real time. Here, we evaluated the utility of using the MV blood flow rate in combination with ME for the diagnosis of EGC as a retrospective study.

Methods: Patients with differentiated-type EGC ($n = 10$) or patchy redness ($n = 10$) underwent ME with blue laser imaging. The mean MV blood flow rates of EGC, patchy redness, and background mucosa were calculated by the mean movement distance of one tagging red blood cell using split images of ME with blue laser imaging videos. We compared the mean MV blood flow rate between EGC, patchy redness, and background mucosa and also calculated the MV blood flow imaging ratio (inside lesion/background mucosa) between EGC and patchy redness.

Results: Mean MV blood flow rate was significantly lower in EGC (1481 $\mu\text{m/s}$; range 1057–1762) than in patchy redness (3859 $\mu\text{m/s}$; 2435–5899) or background mucosa (4140.6 $\mu\text{m/s}$; 2820–6247) ($P < 0.01$). The MV blood flow imaging ratio was significantly lower in EGC (0.39; 0.27–0.62) than in patchy redness (0.90; 0.78–1.1) ($P < 0.01$).

Conclusions: Dynamic diagnosis with MV blood flow rate using ME may be useful for the differential diagnosis of EGC and patchy redness. Endoscopic assessment of dynamic processes within the gastric mucosa may facilitate the diagnosis of EGC.

(ME).^{4–12} Recently, the ME simple diagnostic algorithm for EGC (MESDA-G) has been proposed as a unified system for ME diagnosis of EGC.¹⁰ However, the full potential of MESDA-G requires the expertise of experienced endoscopists. While e-learning may be an effective tool for training staff to make a diagnosis using M-NBI, further development of diagnostic technology in this area is still required.¹³ In clinical practice, distinguishing patients with differentiated-type EGC from patchy redness patients (flat or slightly depressed erythematous lesions that have various shapes, sizes, and red densities in gastric antrum and the atrophic area of gastric body) using endoscopy is sometimes very difficult. This

is problematic in the endoscopic diagnosis of EGC, because the frequency of EGC patients who have undergone *Helicobacter pylori* eradication is increasing in Japan, and most of these patients have patchy redness in the stomach.^{14–19} Therefore, a simple diagnostic method for distinguishing between differentiated-type EGC and patchy redness is required.

Magnifying endoscopy simple diagnostic algorithm for early gastric cancer is used for qualitative diagnosis based on irregularities in the shape, distribution, and arrangement of microvascular (MV) architecture and microsurface structure. However, it is a “static” diagnostic algorithm that uses still images. ME visualizes subepithelial MV red blood cell (RBC) flow in real time, but there have been no studies that have assessed the utility of MV blood flow for diagnosis of EGC. Here, we addressed this gap in our knowledge by developing a new method for measuring the MV blood flow rate of subepithelial microvessels using ME and evaluating its utility for diagnosis of EGC.

Methods

Patients and materials. We retrospectively reviewed M-BLI videos of patients with differentiated-type EGC for preoperative M-BLI examination and patients with patchy redness for screening examination at our hospital between February 2018 and May 2019. To calculate the MV blood flow rate accurately, we randomly selected 20 cases, which one RBC in the microvessels could be tagged reliably inside the lesion and in the surrounding background mucosa. As a result, we enrolled 10 M-BLI videos of patients with differentiated-type EGC and 10 M-BLI videos of patients with patchy redness in whom gastric subepithelial MV blood flow rate was successfully measured by the recorded videos (Fig. 1). In this study, patchy redness was selected as the control group to evaluate the utility of MV blood flow rate in the diagnosis of EGC.

We retrospectively analyzed clinicopathological and endoscopic findings such as age, sex, comorbidities (hypertension), *H. pylori* infection, tumor location, tumor size, macroscopic type, mucosal atrophy, histological type, depth of invasion, lymphovascular invasion, the demarcation line (DL), MV pattern (MVP), and microsurface pattern according to the MESDA-G, white opaque substance (WOS), white grove appearance, and light blue crest.

Endoscopic system and examination. All procedures were carried out with optical magnifying endoscopes (EG-L600ZW7; Fujifilm Corporation, Tokyo, Japan) and the endoscope video system (LASEREO 7000 series; Fujifilm Corporation). In the blue laser imaging mode, the structure enhancement function was fixed at the B6 level, with the color mode fixed at level 1. To obtain well-focused magnifying endoscopic images of the lesion easily, we attached a black soft hood (MAJ-1989; Olympus Medical Systems, Tokyo, Japan) on the tip of the scope and used water immersion technique with maximal magnification during the M-BLI procedure. In addition, we usually used the antiperistaltic agent to obtain well-focused magnifying endoscopic images of the lesion. We selected spraying L-menthol into the stomach or intravenous injection of scopolamine butylbromide or glucagon. The level of maximal magnification was set at high (three white blocks, about 115×) or maximum (four white blocks, 145×) magnifications on 26-in. monitor, and a scale in 1-mm increments was visualized at 115× or 145× magnifications prior to examination (Fig. S1). All endoscopic investigations involving M-BLI were performed by H. U., a skilled endoscopist accredited by the Japan Gastroenterological Endoscopy Society.

Method of microvascular blood flow rate measurement. Figure 2 shows the method used to measure MV blood flow rate. All M-BLI video images were split into 30 fps, and

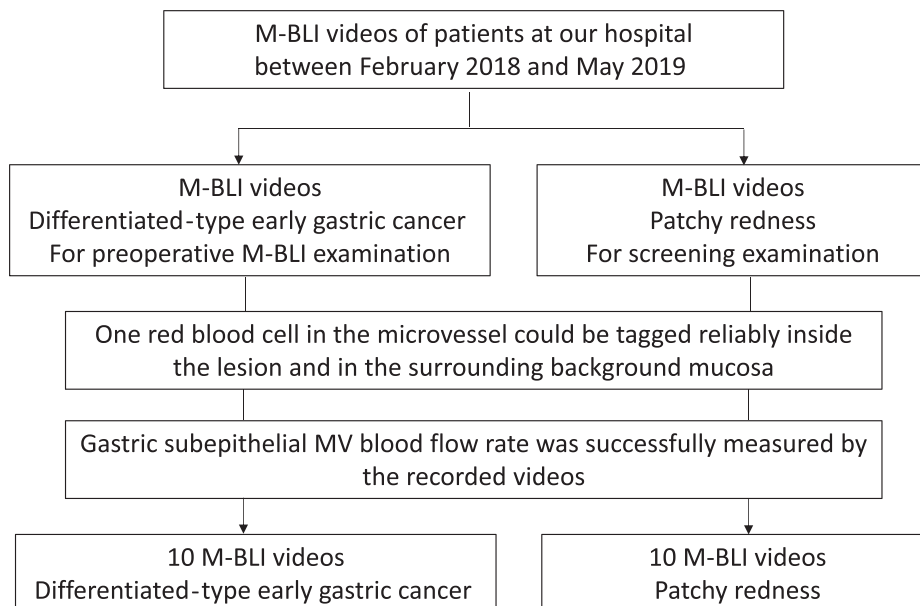


FIGURE 1 Flow diagram of enrolment. M-BLI, magnifying endoscopy with blue laser imaging; MV, microvascular.

the mean MV blood flow rate was calculated by the mean movement distance of one tagging RBC. First, the distance covered by one tagging RBC was measured manually at continuing split images (distance A) on a large screen, and the distance of 1-mm increments (distance B) was also measured manually on the same screen. Second, the mean MV blood flow rate was calculated by distance A, distance B, and the number of frames (mean blood flow rate [$\mu\text{m/s}$] = distance A [μm]/distance B [μm] \times 30 [frames]/number of frames [frames]). Third, the MV blood flow rate was divided by 1.33, which is refractive index of water, because distance A was measured in water and distance B was measured in air. We calculated the mean MV blood flow rate both inside the lesion and in the surrounding background mucosa in all cases.

Objectives. We developed a new method for measuring the MV blood flow rate of subepithelial microvessels using ME and evaluated its utility for the diagnosis of EGC. The primary outcome was to compare MV blood flow rates between three groups: the EGC group, patchy redness group, and background mucosa group. The secondary outcome was to calculate and compare the MV blood flow imaging ratio (inside lesion/background mucosa) between the EGC and patchy redness groups to account for individual differences such as blood pressure.

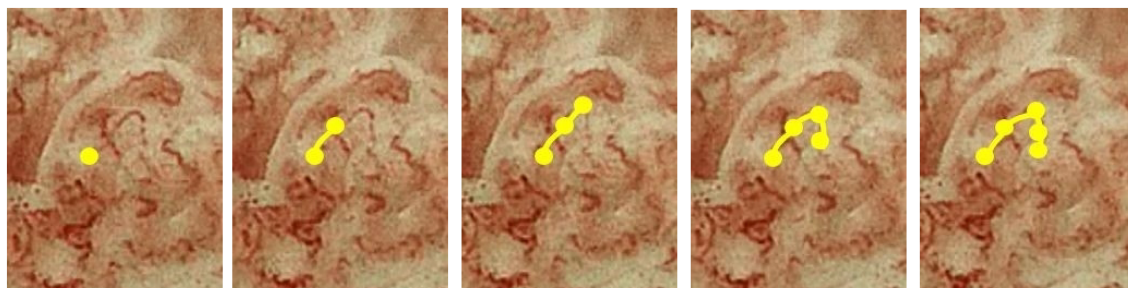
Statistical analysis. All statistical analyses were performed with EZR (Easy R; Saitama Medical Center, Jichi Medical University, Saitama, Japan),²⁰ which is a graphical user interface for R (The R Foundation for Statistical Computing, Vienna, Austria). Continuous data were compared using the Mann–Whitney *U*-test. Categorical analysis of variables was performed using Fisher’s exact test, with $P < 0.05$ considered to indicate a statistically significant difference.

Ethics. This study was reviewed and approved by the Institutional Review Board of Juntendo University School of Medicine (approval number: #20-219). Patients were not required to give consent for the study because the analysis used anonymous clinical data that were obtained after each patient had agreed to endoscopic examination and treatment by verbal and documental consent. Individuals cannot be identified from the data presented.

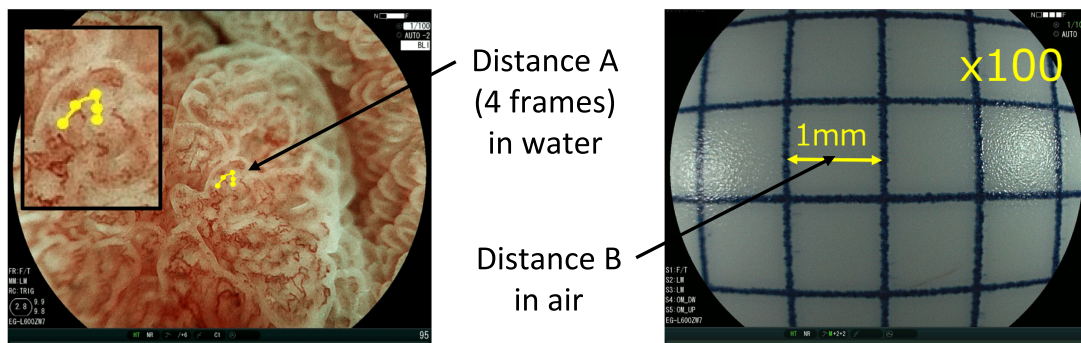
Results

Patient and lesion characteristics. We collected 10 M-BLI videos of patients with differentiated-type EGC (Video S1) and 10 M-BLI videos of patients with patchy redness (Video S2), in whom gastric subepithelial MV blood flow rate could be measured by the recorded videos. Endoscopic images of EGC and patchy redness are shown in Figure 3.

Early gastric cancer



Movement distance of one tagging RBC



$$\text{Mean blood flow rate } (\mu\text{m/sec}) = \frac{\text{Distance A } (\mu\text{m})}{\text{Distance B } (\mu\text{m})} \times \frac{30 \text{ (frames)}}{4 \text{ (frames)}} \div 1.33$$

FIGURE 2 Methodology for the measurement of microvascular blood flow rate. RBC, red blood cell.

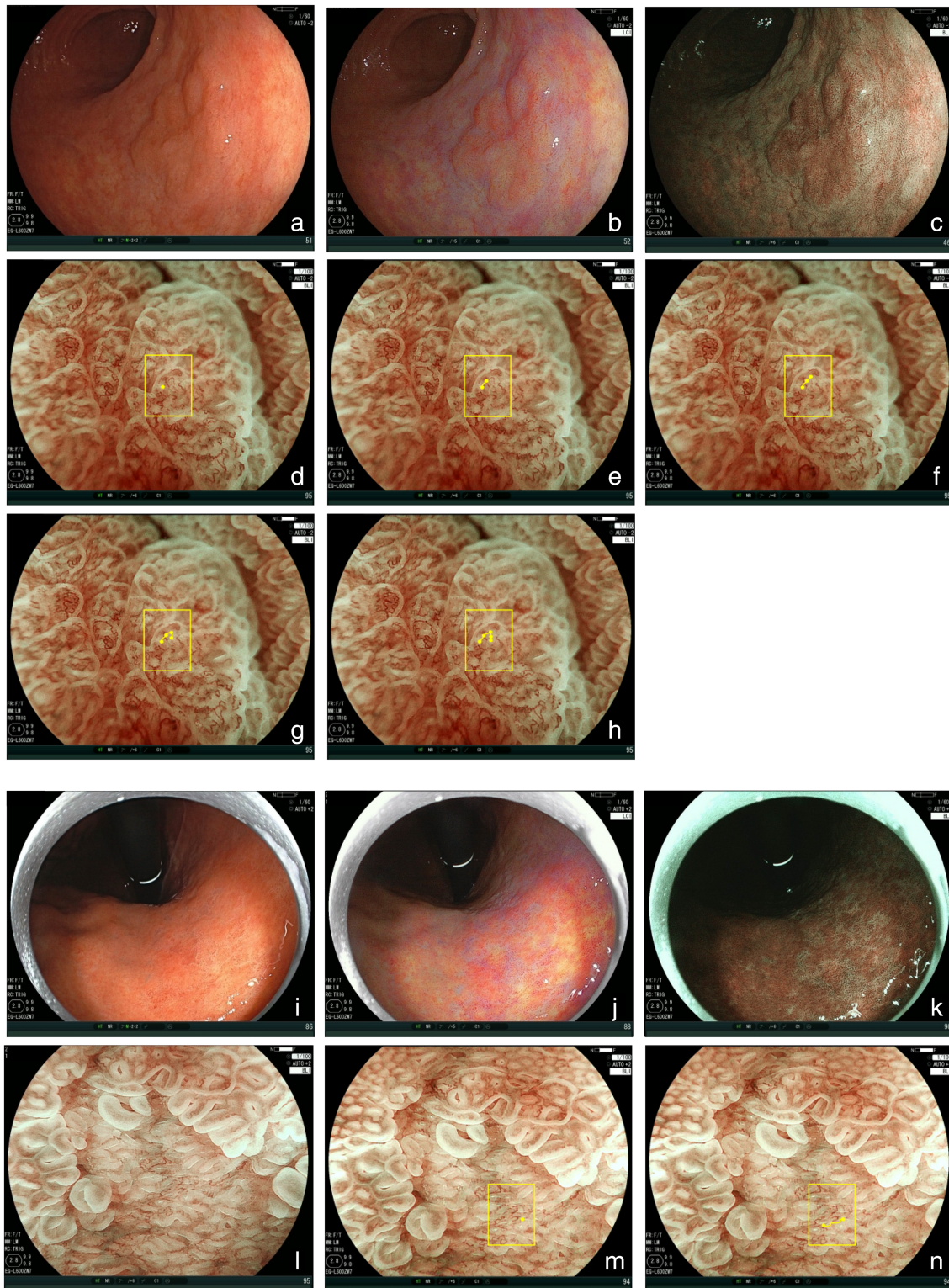


FIGURE 3 Endoscopic images of early gastric cancer and patchy redness. (a–h) Early gastric cancer (case 1). (a) White-light imaging. (b) Linked color imaging. (c) Blue laser imaging. (d–h) Magnifying endoscopy with blue laser imaging. Magnifying endoscopy simple diagnostic algorithm for early gastric cancer: irregular microvascular pattern plus irregular microsurface pattern with a demarcation line. (i–n) Patchy redness (case 4). (i) White-light imaging. (j) Linked color imaging. (k) Blue laser imaging. (l–n) Magnifying endoscopy with blue laser imaging. Magnifying endoscopy simple diagnostic algorithm for early gastric cancer: regular microvascular pattern plus regular microsurface pattern with a demarcation line. Yellow dots and lines represent the movement distance of one tagging red blood cell.

Table 1 Baseline characteristics

	Early gastric cancer <i>n</i> = 10	Patchy redness <i>n</i> = 10
Age (years, range)	73.7 (44–82)	69.7 (54–77)
Sex (male/female)	7/3	7/3
Comorbidities (hypertension)	3 (30%)	4 (40%)
<i>Helicobacter pylori</i> infection (positive/eradicated)	3/7	0/10
Tumor location (U/M/L)	1/3/6	1/1/8
Tumor location (GC/LC/Ant/Post)	3/6/1/0	4/5/1/0
Tumor size (mm)	10 (5–32)	NA
Macroscopic type (elevated/depressed)	5/5	0/10
Mucosal atrophy (C-1,2/C-3, O-1/O-2,3)	0/5/5	0/2/3
Histological type (tub1/tub2)	8/2	NA
Depth of invasion (M/SM)	10/0	NA
Lymphovascular invasion	0 (0%)	NA

Ant, anterior wall; GC, greater curvature; L, lower third; LC, lesser curvature; M, intramucosal layer; M, middle third; NA, not assessed; Post, posterior wall; SM, submucosal layer; tub1, well-differentiated adenocarcinoma; tub2, moderately differentiated adenocarcinoma; U, upper third.

Table 1 shows baseline characteristics of patients with EGC and patchy redness. There were more men than women (7 vs 3, EGC and patchy redness), the mean age was 73.7 and 69.7 years (EGC and patchy redness, respectively), and the prevalence of hypertension was 30% and 40% (EGC and patchy redness, respectively). In most cases, patients had undergone *H. pylori* eradication (i.e. had “post-eradication” status), and lesions were located at the lower third of the stomach. All EGC patients had undergone endoscopic submucosal dissection. The mean tumor size was 10 mm (range 5–32), and macroscopic observation revealed five superficial elevated lesions and five superficial depressed lesions. There were more well-differentiated adenocarcinomas than moderately differentiated adenocarcinomas (eight and two, respectively), and all cancer lesions were intramucosal and had no lymphovascular invasion. Table 2 shows the findings of M-BLI diagnosis of EGC and patchy redness. According to MESDA-G, all EGC lesions were diagnosed as cancer due to the presence of an irregular MVP with a DL, whereas all patchy redness lesions were diagnosed as non-cancer because they had a regular MVP and regular microsurface pattern with a DL. The subepithelial MV blood flow could be visualized even in EGC lesions with WOS, although WOS within the superficial part of the EGC obscures

the microvessels. White grove appearance was observed only in EGC (40%) but not in patchy redness (0%). Light blue crest was observed more often in patchy redness (80%) than in EGC (30%).

Primary outcome. Table 3 shows the MV blood flow rate associated with EGC, patchy redness, and background mucosa. The mean MV blood flow rate was significantly lower in EGC (1481 $\mu\text{m/s}$; range 1057–1762) than in patchy redness (3859 $\mu\text{m/s}$; 2435–5899) or background mucosa (4140.6 $\mu\text{m/s}$; 2820–6247) ($P < 0.01$, Fig. S2). In addition, the mean MV blood flow rate was significantly lower in superficial elevated-type EGC (1244.2 $\mu\text{m/s}$; 1057–1562) than in superficial depressed-type EGC (1717.8 $\mu\text{m/s}$; 1665–1762) ($P < 0.01$). There were no significant differences in MV blood flow rate according to sex, hypertension, *H. pylori* infection status, tumor location, and histological type in each group.

Secondary outcome. Table 3 shows the MV blood flow imaging ratio associated with EGC and patchy redness. The ratio was significantly lower in EGC (0.39; 0.27–0.63) than in patchy redness (0.90; 0.79–1.1) ($P < 0.01$, Fig. S3). However, the ratio was not significantly different between patients with superficial elevated-type EGC (0.35; 0.27–0.43) and those with superficial depressed-type EGC (0.43; 0.30–0.62) ($P = 0.28$). There were no significant differences in MV blood flow imaging ratio according to sex, hypertension, *H. pylori* infection status, tumor location, and histological type in each group.

Discussion

Here, we developed a new method for measuring the MV blood flow rate of subepithelial microvessels using ME. We believe this is the first study to report the analysis of gastric subepithelial MV blood flow rate using ME during the diagnosis of EGC. The flow rate was significantly lower in EGC compared with patchy redness and background mucosa. In addition, the flow rate was significantly lower in patients with superficial elevated-type EGC than in those with superficial depressed-type EGC.

At our hospital, we have used the water immersion technique with maximal magnification. This has yielded excellent diagnostic accuracies for gastric cancer patients with *H. pylori* post-eradication or naïve status; historically, it has been difficult to diagnose gastric cancer in these cases.^{21,22} The technique we used in our study can eliminate halation, thereby generating perfectly focused, clear, and sharp images of uniform quality, which

Table 2 Endoscopic findings of magnifying endoscopy with blue-light imaging

	Early gastric cancer <i>n</i> = 10	Patchy redness <i>n</i> = 10
Demarcation line (present/absent)	100% (10/0)	100% (10/0)
Microvascular pattern (regular/irregular/absent)	0/10/0	10/0/0
Microsurface pattern (regular/irregular/absent)	0/7/3	10/0/0
MESDA-G (cancer/non-cancer)	10/0	0/10
White opaque substance (present/absent)	6/4	0/10
White grove appearance (present/absent)	4/6	0/10
Light blue crest (present/absent)	3/7	8/2

MESDA-G, magnifying endoscopy simple diagnostic algorithm for early gastric cancer.

Table 3 Microvascular blood flow rate and microvascular blood flow imaging ratio

			Microvascular blood flow rate ($\mu\text{m/s}$)		
			Early gastric cancer and patchy redness	Background mucosa	Microvascular blood flow imaging ratio
1	Early gastric cancer	Elevated type	1057	2820	0.37
2	Early gastric cancer	Elevated type	1269	3383	0.38
3	Early gastric cancer	Elevated type	1222	2820	0.43
4	Early gastric cancer	Elevated type	1562	4859	0.32
5	Early gastric cancer	Elevated type	1111	4164	0.27
6	Early gastric cancer	Depressed type	1762	2820	0.62
7	Early gastric cancer	Depressed type	1762	3525	0.5
8	Early gastric cancer	Depressed type	1665	5553	0.3
9	Early gastric cancer	Depressed type	1735	4511	0.38
10	Early gastric cancer	Depressed type	1665	4720	0.35
1	Patchy redness		3525	3877	0.91
2	Patchy redness		3172	3525	0.9
3	Patchy redness		3102	2820	1.1
4	Patchy redness		3383	3665	0.92
5	Patchy redness		2435	2820	0.86
6	Patchy redness		3609	4164	0.87
7	Patchy redness		4859	6247	0.78
8	Patchy redness		5899	6247	0.94
9	Patchy redness		4164	5274	0.79
10	Patchy redness		4442	4997	0.89
	Early gastric cancer (mean \pm SD)		1481 \pm 283.9	—	0.39 \pm 0.103
	Patchy redness (mean \pm SD)		3859 \pm 1003.8	—	0.90 \pm 0.089
	Background mucosa (mean \pm SD)		—	4140.6 \pm 1129.1	—

are suitable for endoscopic diagnosis. These videos are therefore optimal for measuring the MV blood flow rate. As shown in the videos, it is critical to approach the lesion without applying pressure in order to measure the MV blood flow rate accurately. This is because pressing the lesion with a scope can have a profound effect on the MV blood flow rate.

Magnifying endoscopy can visualize the subepithelial capillary network, collecting venules, and subepithelial microvessels. The term “subepithelial microvessels” should be applied when the vessels cannot be categorized as either a capillary or a venule in a pathological condition.²³ In this study, we could visualize the blood flow of the subepithelial microvessels both inside the lesion and in the background mucosa of the lesion. The subepithelial microvessels are located at the subepithelial area of the mucosal layer extend 100 μm down from the surface. The average blood velocity of capillaries, which are the smallest blood vessel type, is 300–1000 $\mu\text{m/s}$.²⁴ An RBC is about 7–8 μm wide, and the width of capillaries is between 5 and 15 μm . Therefore, RBCs must undergo deformation, tumbling, or tank treading to pass through the narrowest part of the capillaries. In addition, blood flow rate is not constant, because it is affected by blood pressure, pulsatility index, and the elasticity and mobility of the blood vessel wall. Although it is challenging to generate an accurate mathematical description of blood flow rate, we did notice in the M-BLI videos that RBCs seem to move and stop repeatedly (Videos S1 and S2). The blood flow rate we report in this study (range: 1057–6247 $\mu\text{m/s}$) was faster than the average blood velocity in capillaries (range: 300–1000 $\mu\text{m/s}$). This may be because we calculated the average of the maximum speed of one RBC while

the RBC was moving. In addition, regarding the variation in blood flow rate of each microvessel within the same region, the MV blood flow rate of one representative microvessel was measured in this study, because there was no significant difference in the MV blood flow rate of each microvessel within the same region in some EGC and patchy redness cases (data not shown).

The mean MV blood flow rate was significantly lower in EGC than in patchy redness or background mucosa. Additionally, the rate was significantly lower in superficial elevated-type EGC than in superficial depressed-type EGC. In general, ME assigns the microvessels in EGC with an irregular morphology due to the presence of caliber change, meandering, branch architecture, asymmetric distribution, and distorted arrangement. Histopathologically, the density of tumor glands around the microvessels is higher than it is around normal gastric glands, and the structure of tumor glands is irregular (Fig. 4b–d). The stromal structure around the tumor glands where microvessels are running is complex and narrow (Fig. 4c). Therefore, we hypothesized that the difference in caliber and tortuosity of microvessels and the high density of tumor glands around the microvessels may be associated with lower gastric subepithelial MV blood flow rate in EGC compared with noncancerous lesions such as patchy redness and background mucosa. The density of tumor glands in superficial elevated-type EGC was higher than that of superficial depressed-type EGC, although the caliber and tortuosity of microvessels were similar in each (Fig. 4a,c,e,g). In summary, MV blood flow rate in the stomach may be affected by caliber change and tortuosity of microvessels and the density of gastric glands around the microvessels. However, further research

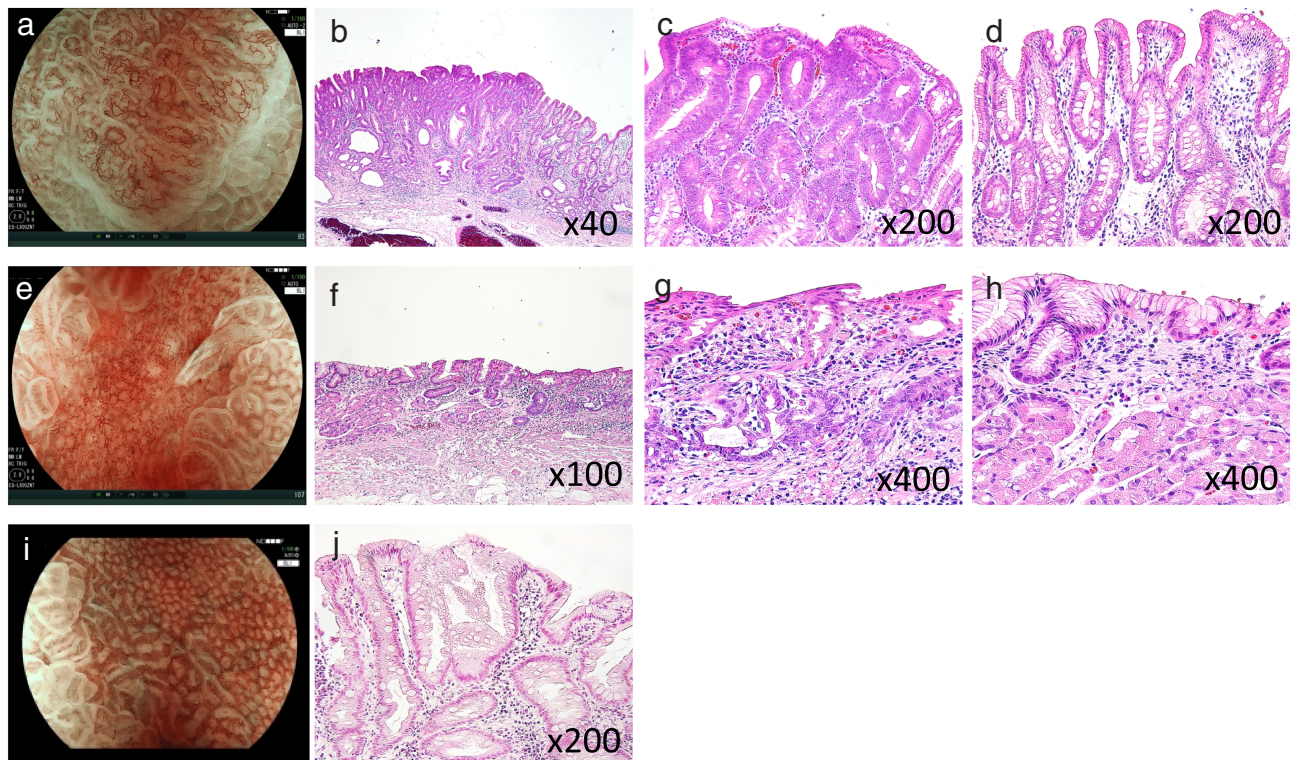


FIGURE 4 Pathological findings on the surface of early gastric cancer, patchy redness, and background mucosa. (a–d) Superficial elevated-type early gastric cancer (case 1). (a) Magnifying endoscopy with blue laser imaging. (b–d) Pathology (hematoxylin and eosin). (c) Pathology of the surface of early gastric cancer. (d) Pathology of the surface of background mucosa. The tumor gland density in early gastric cancer was higher than that of gastric glands in background mucosa; the tumor glands had an irregular structure. The stromal structure around the tumor glands was complex and narrow. (e–h) Superficial depressed-type early gastric cancer (case 7). (e) Magnifying endoscopy with blue laser imaging. (f–h) Pathology (hematoxylin and eosin). (g) Pathology of the surface of early gastric cancer. (h) Pathology of the surface of background mucosa. The density of tumor glands in early gastric cancer was a little higher than that of gastric glands in background mucosa, and the structure of tumor glands was irregular. The stromal structure around the tumor glands showed complex and slightly narrow. (i, j) Patchy redness. (i) Magnifying endoscopy with blue laser imaging. (j) Pathology of the surface of patchy redness. The density of gastric glands in patchy redness was low, and the structure of gastric glands was regular. The stromal structure was sparse and therefore similar to that observed in the background mucosa (d–h).

(including studies that examine fluid mechanics and elastic mechanics) is needed in order to elucidate the factors that regulate MV blood flow rate in the gastric mucosa.

Dynamic endoscopy diagnosis of the biological functions of gastrointestinal mucosa may offer a new approach for the diagnosis and etiological elucidation of various gastrointestinal diseases. To move this out of the proof-of-concept phase for EGC diagnosis, studies designed to test whether MV blood flow rate can be measured in real time in the clinic are required. A positive outcome from such studies would pave the way for ME-guided evaluation of other physiological processes such as inflammation, gastric movement, and mucus secretion.

This study has several limitations. First, it was exploratory in nature and only focused on differentiated-type EGC *versus* patchy redness. In follow-up studies, we will investigate the MV blood flow rate in additional types of gastric lesion and also elucidate the pathophysiological processes that underlie the lower MV blood flow rate in EGC when compared with noncancerous lesions. Second, the present study was retrospective and based on a small number of patients from a single center. Furthermore, we could not completely eliminate selection bias, even though

the M-BLI videos were extracted at random for our analysis. In the future, a prospective multicenter comparative study with a large sample size that analyzes interrater agreement should be conducted. Third, in some cases, MV blood flow cannot be visualized by ME. This can be because the microvessels themselves are not visible at the surface or because RBC flow appears to stop even when microvessels are visible. Fourth, we did not specify which area of the lesion to measure MV blood flow rate and at what moment MV blood flow was measured. We plan to analyze after defining strict criteria for the site and timing of MV blood flow measurement. Fifth, because the microvessels in the cancerous mucosa usually show three-dimensional disorganized MV architecture, if the microvessels run vertically, the blood flow, which was measured on the surface in two dimensions, may become slow. Sixth, patchy redness and the surrounding background mucosa were subjected only to endoscopic diagnosis, not to biopsy. However, because the endoscopist in charge of image capturing is experienced physician, any lesions suspected of cancer, even in the slightest, would have been subjected to biopsy examination. Because no such images were included in this study, there was considered to be little chance that images of cancer were

mixed in by mistake. Thus, we believe the diagnostic quality of this study.

In conclusion, we have developed a new method for measuring the MV blood flow rate of subepithelial microvessels using ME in the stomach. Using this methodology, we found that EGC was associated with a significantly lower gastric subepithelial MV flow rate compared with that of patchy redness and the background mucosa. Endoscopic assessment of the dynamic functions of gastric mucosa may offer a novel approach in the diagnosis of EGC. We hope that translation of this strategy to ME-driven diagnosis of EGC in daily clinical practice will become reality in the near future.

References

- Hamashima C, Okamoto M, Shabana M *et al.* Sensitivity of endoscopic screening for gastric cancer by the incidence method. *Int. J. Cancer* 2013; **133**: 653–9.
- Osawa H, Yamamoto H. Present and future status of flexible spectral imaging color enhancement and blue laser imaging technology. *Dig. Endosc.* 2014; **26**: 105–15.
- Gono K, Yamazaki K, Douguchi N *et al.* Endoscopic observation of tissue by narrow band illumination. *Op. Rev.* 2003; **10**: 211–5.
- Yao K, Anagnostopoulos GK, Ragnath K. Magnifying endoscopy for diagnosis and delineating early gastric cancer. *Endoscopy* 2009; **41**: 462–7.
- Yao K, Iwashita A, Tanabe H *et al.* Novel zoom endoscopy technique for diagnosis of small flat gastric cancer: a prospective, blind study. *Clin Gastroenterol Hepatol* 2007; **5**: 869–78.
- Kato M, Kaise M, Yonezawa J *et al.* Magnifying endoscopy with narrow-band imaging achieves superior accuracy in the differential diagnosis of superficial gastric lesions identified with white-light endoscopy: a prospective study. *Gastrointest Endosc* 2010; **72**: 523–9.
- Ezoe Y, Muto M, Uedo N *et al.* Magnifying narrowband imaging is more accurate than conventional white-light imaging in diagnosis of gastric mucosal cancer. *Gastroenterology* 2011; **141**: 2017–25.
- Yao K, Doyama H, Gotoda T *et al.* Diagnostic performance and limitations of magnifying narrow-band imaging in screening endoscopy of early gastric cancer: a prospective multicenter feasibility study. *Gastric Cancer* 2014; **17**: 669–79.
- Yamada S, Doyama H, Yao K *et al.* An efficient diagnostic strategy for small, depressed early gastric cancer with magnifying narrow-band imaging: a post-hoc analysis of a prospective randomized controlled trial. *Gastrointest Endosc* 2014; **79**: 55–63.
- Muto M, Yao K, Kaise M *et al.* Magnifying endoscopy simple diagnostic algorithm for early gastric cancer (MESDA-G). *Dig. Endosc.* 2016; **28**: 379–93.
- Dohi O, Yagi N, Yoshida S *et al.* Magnifying blue laser imaging versus magnifying narrow-band imaging for the diagnosis of early gastric cancer: a prospective, multicenter, comparative study. *Digestion* 2017; **96**: 127–34.
- Dohi O, Yagi N, Majima A *et al.* Diagnostic ability of magnifying endoscopy with blue laser imaging for early gastric cancer: a prospective study. *Gastric Cancer* 2017; **20**: 297–303.
- Nakanishi H, Doyama H, Ishikawa H *et al.* Evaluation of an e-learning system for diagnosis of gastric lesions using magnifying narrow-band imaging: a multicenter randomized controlled study. *Endoscopy* 2017; **49**: 957–67.
- Toyoshima O, Nishizawa T, Koike K. Endoscopic Kyoto classification of *Helicobacter pylori* infection and gastric cancer risk diagnosis. *World. J. Gastroenterol.* 2020; **26**: 466–77.
- Cho J-H, Jeon SR, Jin S-Y *et al.* Clinical applicability of gastroscopy with narrow-band imaging for the diagnosis of *Helicobacter pylori* gastritis, precancerous gastric lesion, and neoplasia. *World J Clin Cases* 2020; **8**: 2902–16.
- Majima A, Handa O, Naito Y *et al.* Early-stage gastric cancer can be found in improved atrophic mucosa over time from successful *Helicobacter pylori* eradication. *Digestion* 2017; **95**: 194–200.
- Kodama M, Okimoto T, Mizukami K *et al.* Endoscopic and immunohistochemical characteristics of gastric cancer with versus without *Helicobacter pylori* eradication. *Digestion* 2018; **97**: 288–97.
- Kobayashi M, Hashimoto S, Nishikura K *et al.* Magnifying narrow-band imaging of surface maturation in early differentiated type gastric cancers after *Helicobacter pylori* eradication. *J. Gastroenterol.* 2013; **48**: 1332–42.
- Saka A, Yagi K, Nimura S. Endoscopic and histological features of gastric cancers after successful *Helicobacter pylori* eradication therapy. *Gastric Cancer* 2016; **19**: 524–30.
- Kanda Y. Investigation of the freely available easy-to-use software ‘EZR’ for medical statistics. *Bone Marrow Transplant* 2013; **48**: 452–8.
- Akazawa Y, Ueyama H, Yao T *et al.* Usefulness of demarcation of differentiated-type early gastric cancers after *Helicobacter pylori* eradication by magnifying endoscopy with narrow-band imaging. *Digestion* 2018; **98**: 175–84.
- Matsumoto K, Ueyama H, Yao T *et al.* Diagnostic limitations of magnifying endoscopy with narrowband imaging in early gastric cancer. *Endosc Int Open* 2020 in press.
- Yao K. Clinical application of magnifying endoscopy with narrow-band imaging in the stomach. *Clin. Endosc.* 2015; **48**: 481–90.
- Marieb EN, Hoehn K. The cardiovascular system: blood vessels. In: *Human Anatomy & Physiology*, 9th edn. Pearson Education, 2013; 712 ISBN 978-0-321-74326-8.

Supporting information

Additional supporting information may be found online in the Supporting Information section at the end of the article.

Figure S1. A scale in 1-mm increments at 100x and 135x magnifications.

Figure S2. Microvascular blood flow rate (early gastric cancer vs. patchy redness vs. background mucosa).

Figure S3. Microvascular blood flow imaging ratio (early gastric cancer vs. patchy redness).

Video S1. Magnifying endoscopy with blue laser imaging of early gastric cancer and the background mucosa (normal and slow motion (30%) video).

Video S2. Magnifying endoscopy with blue laser imaging of patchy redness and the background mucosa (normal and slow motion (30%) video).